SCREENING EFFECTS IN RELATIVISTIC MODELS OF DENSE MATTER AT FINITE TEMPERATURE

Joaquín Diaz-Alonso[1,3], Armando Pérez[2] and Horacio D. Sivak[1]
[1] *D.A.R.C., Observatoire de Paris-Meudon, UPR 176 CNRS F-92195 Meudon, France.*
[2] *Departamento de Física Teórica, Universidad de Valencia E-46100 Burjassot (Valencia) Spain.*
[3] *Departamento de Física, Universidad de Oviedo E-33007 Oviedo, Spain.*

We investigate screening effects of the medium on the potential interaction between two static 'charges' for different models of dense plasmas in the one-boson exchange approximation. The potential can exhibit an oscillatory behavior, which is related to the analytic structure of the corresponding boson propagators in the complex q-plane. We have first revisited the one-pion exchange in a nuclear medium. In addition to Friedel oscillations, which are associated to branch cuts in the q-plane, there appears another oscillatory component, which arises from a pole on the pion propagator. This pole is located appart from the axes, giving rise to an oscillating Yukawa-like potential. Therefore, we call this phenomenon 'Yukawa oscillations'. This phenomenon does not appear in the Debye component of the QED screened potential, even if the coupling constant is artificially increased. We have also studied a model of QCD quark-gluon plasma. In this case, the one-gluon propagator also shows this kind of poles. At high densities and/or temperatures, where one expects perturbative QCD to be valid, the pole shifts towards large momenta.

I. INTRODUCTION

The natural framework for the analysis of high-density matter under conditions where relativistic effects are essential is Quantum Field Theory [1], where dense plasmas are described (at fundamental or phenomenological level) as assemblies of fermions (electrons, nucleons, quarks, etc...) interacting through the exchange of bosons (photons, mesons, gluons, etc...). The dynamics of these systems is defined by Lagrangian models whose solution (in general, in a given approximation), allows for the calculation of macroscopic properties. One interesting issue which can be obtained from the Lagrangian (using, for example, the one-boson exchange approximation "OBE") is the description of the two-body interaction in vacuum, in terms of a phenomenological potential. Simple instances are the Coulomb and Yukawa potentials associated, respectively, to the exchange of massless and massive bosons.

A consequence of the collective behavior in a plasma is the appearance of screening effects on the two-body interaction. In a classical electromagnetic plasma, the Coulomb-like interaction between two static charges in vacuum becomes, when modified by the medium, the exponentially damped Debye interaction. However, in degenerate quantum electromagnetic plasmas the in-medium potential becomes long-ranged and oscillatory, both in the non-relativistic [2] and relativistic [3], [4] cases. These so-called Friedel oscillations have observable consequences [5].

The phenomenological description of the nuclear interaction in vacuum through the exchange of massive mesons [1] leads, in the static OBE approximation, to an interparticle potential which is exponentially damped with the distance [7]. The effects of the medium in a degenerate nuclear plasma, as obtained in the same approximation [8], or in a direct calculation of the interaction energy [9], introduce qualitative modifications on the two-particle interaction potential, which becomes long-ranged and oscillatory, as in the case of the degenerate electromagnetic plasma. The analysis of the screened potential in both cases allows for a separation into two components: a Friedel-like component, which is damped as a power of the distance and dominates the long range, and an exponentially damped Yukawa-like (or Debye-like in QED) component. We must stress, however, that there are qualitative differences between this Yukawa component and the Debye screening of QED: the first one is, in fact, oscillatory below some critical temperature, whereas not such oscillations are present in the Debye component in the QED plasma. Friedel oscillations, which are present in both cases, fade away for lower temperatures [9]. As we will discuss later, these *Yukawa oscillations* are also present in other physical systems such as a quark-gluon plasma, for which Kapusta et al. [10] have been evidenced the existence of Friedel oscillations.

[1] In the standard terminology, this approach is known as 'Quantum Hadrodynamics' or QHD [6].

The analytic structure of the dressed propagators governs the behavior of the screened potential [9]. From the mathematical point of view, Friedel oscillations are associated to the Kohn singularity [11] in the matter part of the zero-temperature polarization tensor, which shows branch cuts starting at a transferred momentum $q = \pm 2p_f$, where p_f is the Fermi momentum of fermions in the plasma. On the other hand, Yukawa oscillations are associated to a pole of the propagator in the complex q -plane which has a non-vanishing real part, in contrast to Debye screening, which arises from a pole on the imaginary axis.

In this paper we analyze the two-particle interaction in dense plasmas, using the above mentioned models. Here we are not interested in a precise quantitative description of actual dense matter using more or less adapted theoretical models. Our main concern is rather to evidence the above mentioned characteristics of the screening, as a result from basic properties which seem to be present in some relativistic models describing dense matter and, eventually, to discuss the limitations of such models.

The ground states of the plasma in the electromagnetic and in the quark-gluon cases are described as relativistic free Fermi gases in thermodynamical equilibrium. For the QHD nuclear plasma, the ground state is described by the relativistic Hartree approximation (RHA) [12], which defines the thermodynamics at finite temperature and includes the contributions of vacuum fluctuations. The propagators of the exchanged bosons which are necessary to obtain the screened potential are dressed by the medium. Their expressions have been obtained in a self-consistent one-loop approximation, where matter polarization contributions were calculated at finite temperature and vacuum polarization contributions were included. Such approximation, for QHD, is the first order of a kinetic cluster expansion around the relativistic Hartree ground state [13,14] and coincide at $T = 0$ with the usual one-loop approximation [15].

This paper is organized as follows. In section 2 we introduce the essential equations which are necessary for the analysis of the screening in the models. In section 3 we study the analytic structure of the meson propagators and the oscillatory behavior of the screened potentials. We conclude in section 4 with a discussion on the eventual manifestations in actual systems of the phenomena found here.

II. BASIC EQUATIONS

The static two-particle interaction potential in the medium can be obtained from a linear response analysis, and can be put under the general form [10]:

$$V(r) \;=\; \frac{Q_1 Q_2}{4\pi^2 r} Im \int_{-\infty}^{\infty} dq \frac{q e^{iqr}}{q^2 + F(\omega = 0, q)} \tag{1}$$

Here, r is the distance between the positions of the interacting particles, Q_1 and Q_2 their corresponding "charges" and $k = (\omega, \vec{q})$ the transferred four-momentum. A similar expression can be derived from the OBE approximation in the static ($\omega = 0$) limit [8]. Then, $G(k) = \frac{-1}{-k^2 + F(k)}$ corresponds to the boson propagator, and $F(k)$ is related to the boson self-energy.

To be more explicit, we need to consider each case separately. As representative of QHD, we will study the one-pion exchange. In this case, one has to replace $Q_1 Q_2 \rightarrow -g_\pi^2$, with g_π the pion-nucleon coupling constant, and take into account the pion mass. This means that the pion propagator $G_\pi(\omega \;=\; 0, \vec{q})$ must be written as :

$$G_\pi(\omega \;=\; 0, \vec{q}) = -\frac{1}{q^2 + m_\pi^2 - g_{\sigma\pi} m_\sigma < \sigma > -g_\pi^2 \Pi_\pi(q)} \tag{2}$$

where $\Pi_\pi(k)$ is the pion polarization, which can be decomposed into a matter and a renormalized vacuum contribution $\Pi_\pi(k) \;=\; \Pi_\pi^{mat}(k) \;+\; \Pi_\pi^{vac}(k)$ and m_π is the pion mass. We have included a pion-sigma coupling term in the Lagrangian, as in [9], with $g_{\sigma\pi} = 3.77$. Finally, $m_\sigma = 550$ MeV represents the σ-meson mass and $< \sigma >$ the self-consistent mean-field value of this meson field. The renormalized vacuum contribution to the pion polarization is given by:

$$\begin{aligned} \Pi_\pi^{vac}(k) = \; & (2\pi)^{-2}\{-ak^2 \log\left(\frac{1+a}{1-a}\right) \;+\; k^2 \;-\; m_\pi^2 \;+\; 2(m^2 \;-\; M^2) \\ & -\; 2(k^2 \;-\; 2M^2)\log(\frac{M}{m}) - \; 4(m \;-\; M)^2(1 \;+\; a_0^{-2}) \;-\; (\frac{2}{a_0})\arctan(\frac{1}{a_0}) \\ & \times \left[2(m \;-\; M)^2(1 \;+\; a_0^{-2}) \;+\; k^2(1 \;-\; \frac{2m^2}{m_\pi^2}) \;-\; 2M^2\right]\} \end{aligned} \tag{3}$$

where $a \;=\; \sqrt{1 \;-\; 4M^2/k^2}$, $a_0 \;=\; \sqrt{4m^2/m_\pi^2 \;-\; 1}$ and M is the nucleon effective mass, calculated in the Hartree approximation. In the next section we give the expression for the matter contribution.

From the expression (1) we see that the analytic structure of the propagators on the $\omega \;=\; 0$ axis becomes the essential magnitude which governs the behavior of the screening. In the QHD case there are poles of the propagator on this axis associated to the "tachyonic" branches, which come from the vacuum polarization terms [16]. Such poles arise at large momentum transfer, where the internal structure of the nucleon invalidates the point-particle approach of the model and thus, the effect of this pole on the calculated in-medium potential is spurious. We can try to account phenomenologically for the nucleon structure by the introduction of monopolar form factors $ff(k)$ on the vertex of the loop expansion and the OBE diagrams. To do this we have to replace, in the previous equations

$$\begin{aligned} g_\pi^2 &\rightarrow g_\pi^2 ff(k) \\ ff(k) &= (\Lambda_\pi^2 \;-\; \mu_\pi^2)/(\Lambda_\pi^2 \;-\; k^2) \end{aligned} \tag{4}$$

where Λ_π is a cut-off parameter. When the value of this parameter is properly chosen, the spurious "tachyonic" branches (and the associated pole of the propagator on the $\omega = 0$ axis) disappear. Of course, one could also eliminate the poles associated to these branches by simply discarding the renormalized vacuum

polarization contribution. However, this contribution is essential in obtaining the physical propagation modes. If neglected, new unphysical space-like modes (which introduce new poles in the propagators at small q) are present and can not be eliminated by form factors [16]. The standard expression of the form factors Eq. (4) fits well the known data in vacuum [7]. At finite density and temperature the form factor is expected to be modified by the medium. In a simple bag-model picture the nucleons "swell" as density increases (EMC effect), due to a reduction of the bag pressure. Higher-order calculations of the vertex function [17], where the surrounding meson cloud defines the size of the nucleon, leads to a similar behavior. Here we shall keep the form factor unchanged in the medium according to our level of approximation, but it must be emphasized that, in an improved calculation, the above mentioned effect will cause a stronger suppression of high-momentum exchanges at larger densities. Nevertheless, these modifications would affect the short-range part of the interaction, and will not modify our main conclusions, which concern the long-range behavior of the screened potential.

We will also analyze the one-gluon exchange screened potential on a color-singlet state of a quark-antiquark pair. For this analysis, we have considered a $SU(N)$ quark-gluon plasma with N_f quark flavors. One has to replace

$$Q_1 Q_2 \to -\frac{(N^2-1)g^2}{2N} \tag{5}$$

in this case in Eq. (1), where g will be the coupling constant. In order to simplify our analysis , we have restricted ourselves to a plasma with only u and d massless quarks with the same chemical potential. The denominator in Eq. (1) is then related to the one-loop gluon polarization in the static limit. The corresponding formulae can be found, for example, in [18], [19] and [20]. We will write explicit expressions for zero temperature in the next section.

III. ANALYSIS OF THE IN-MEDIUM INTERACTIONS.

As discussed in the previous section, in the case of the pion-nucleon plasma, one has to evaluate Eq.(1) with the quasi-pion propagator given by Eq.(2) and the introduction of the form factors given by the replacement (4). The integration can be transformed to a contour integral in the complex q-plane by analytical continuation of $\Pi(q) \equiv \Pi(\omega = 0, q)$. Let us first discuss the situation at zero temperature. We will summarize the main results found in [9]. The matter contribution can be written as:

$$\Pi_\pi^{mat}(q) = -(2\pi)^{-2}\left[4\varepsilon_f p_f - \left(4M^2+2q^2\right)\log\left(\frac{\varepsilon_f+p_f}{M}\right) + 2\varepsilon_f q \log\left(\frac{q-2p_f}{q+2p_f}\right) + aq^2\log\left(\frac{ap_f+\varepsilon_f}{ap_f-\varepsilon_f}\right)\right] \tag{6}$$

Now $a = \sqrt{1+4M^2/q^2}$ (we have corrected two misprints appearing in Eq.(4.8) of reference [9]). One has on the upper-half plane the analytical structure of the pion propagator shown in Fig. 1a)[2], where we have also shown the contour path to be used in evaluating the integral Eq. (1) . The branch cuts starting at $q = \pm 2p_f$ appear from the logarithms in Eq.(6) and have their origin on the sharp form of the Fermi surface in momentum space at $T = 0$. They give rise to Friedel oscillations. For the nuclear plasma, they could manifest as an instability of the uniform configuration in the Hartree approximation, thus allowing for the possibility of new phases in nuclear matter [21], [22]. Alternatively to the use of contour integrals, one can integrate by parts Eq. (1) , following a systematic method given by Lighthill [23] ; then one finds that $\Pi_\pi^{mat}(q)$ has a pole on the second derivative : the Kohn singularity [11]. In addition to this, one has the pole contributions at the points $q = \pm q_r + iq_i$ shown in Fig. 1a) as the small crosses with a circular contour around them, which we will refer to as the *Yukawa pole*. Then the potential $V(r)$, for large r will consist on two terms :

[2] Aside the branch cuts at $q = \pm 2p_f$, there are also branch cuts at $q = \pm 2iM$ (not shown in the figure). They correspond to the thereshold of particle-antiparticle production. However, they will contribute only for the short-distance range ($r \lesssim 1fm$). Here, we will neglect this contribution.

$$V(r \to \infty) \sim V_F(r) \; + \; V_Y(r) \tag{7}$$

The first component $V_F(r)$ is the Friedel component, which is oscillatory and decays as a power-law of r for large distances, while $V_Y(r)$ is the oscillatory exponentially-damped term (Yukawa term), which has the form :

$$V_Y(r) \; = \; A\frac{1}{r}\sin(q_r r)e^{-q_i r} \tag{8}$$

where the amplitude A, the "effective" pion mass q_i and the "frequency" q_r depend on the plasma density. At low densities, the frequency q_r becomes imaginary and the oscillation disappears. When density vanishes this component reduces to the usual Yukawa potential [9].

We will now discuss the situation for finite temperature. At non-zero temperature T, the Fermi surface is spread over a thickness T and the Kohn singularity disappears. However, at small temperatures the second derivative in the polarization $\Pi_\pi(q,T)$ keeps still an important jump around $q \; = \; \pm 2p_f$. This can be seen in Fig. 2, where we have plotted the second derivative of the polarization as a function of q/m, for various temperatures at saturation density (which corresponds to $p_f \simeq 0.3m$). We see the Kohn singularity at $T \; = \; 0$ and the evolution of the jump around $q \; = \; 2p_f$ as temperature increases. For temperatures around 20 MeV the propagator is a smooth function of q.

At low but finite temperatures ($(\varepsilon_f \; - \; M)/T \gg 1$), with ε_f the nucleon Fermi energy, the Friedel potential becomes

$$V_F(r,T) \approx B(Tp_f^2/r^2)/\nu^2(2p_f,T)\cos(2p_f r)/\sinh(\frac{2\pi r T\varepsilon_f}{p_f}) \tag{9}$$

where

$$\nu(q,T) \; = \; (q^2 \; + \; \Lambda_\pi^2)(q^2 \; + \; m_\pi^2) \; - \; g_\pi^2(\Lambda_\pi^2 \; - \; m_\pi^2)\Pi_\pi(q,T) \tag{10}$$

and B is a constant. In the limit $T \; = \; 0$, Eq.(9) behaves as

$$V_F(r) \; \approx \; cos(2P_f r)/r^3 \tag{11}$$

As temperature increases, the Friedel component is exponentially reduced with T (see Eq.(9)). In the present pion-nucleon model this component fades away, at saturation density, as temperature approaches $T \sim 20MeV$.

The oscillations associated to the Yukawa component are present up to $T \sim 60MeV$. We have shown this behavior in the next figures, where we plot the real part q_r (Fig. 3) and the imaginary part q_i (Fig. 4) of the Yukawa pole, both in units of the free nucleon mass m as a function of the temperature, for three values of the density, defined by a given p_f at $T = 0 : \; p_f = 0.3$, corresponding to saturation density (solid line), $p_f = 0.35$ (dotted line) and $p_f = 0.4$ (dashed line). As it is readily seen, the pole shifts towards the imaginary axis as temperature increases, and remains as a pure imaginary pole for temperatures above some critical value T_c, which depends on the density. As a consequence, Yukawa oscillations are present only if $T < T_c$. This transition can also be presented, from a formal point of view, as q_r 'becoming imaginary'(and negative), thus being effectively substracted from the value of q_i and producing the kink observed on Fig. 4.

Now the question is wether the Yukawa pole found in the pion propagator is a peculiarity of this model or not. We have performed a similar study for the screened photon propagator in QED and the screened gluon propagator in QCD. In the first case, we found a pole on the imaginary axis for all the values of the density and temperature we considered. Of course, this imaginary pole corresponds to the well-known Debye screening phenomenon. An important difference with QHD is the strength of the coupling constant : in QED one has $\alpha = \frac{1}{137}$, whereas for the pion-nucleon model it is much larger ($\frac{g_\pi^2}{4\pi} \sim 14$). We have artificially increased the value of the QED coupling constant, by taking values $\alpha \sim 10$ in order to test if the Yukawa pole arises in QHD as a consequence of the large value of the coupling constant. However, even in this case, we have not found such pole in the electromagnetic case. Therefore we conclude that

the strength of the coupling constant is not the main reason for the appearance of Yukawa oscillations, and they must be instead related to the nature of the model.

The situation is completely different in QCD. Let us consider the gluon propagator at the one-loop approximation, for the model described in the previous section. The denominator in Eq.(1) can be written as :

$$D(q) \equiv q^2 + F(q) = q^2 + F^{mat}(q) + F^{vac}(q) \tag{12}$$

where $F^{mat}(q)$ and $F^{vac}(q)$ stand for the matter and vacuum contributions, respectively. We follow the formulae given in [10] to write these contributions (calculations in this reference are made using the temporal axial gauge). At zero temperature, the matter term is given by

$$F^{mat}(q) = \frac{g^2}{48\pi^2} N_f \left[16p_f^2 + \frac{2p_f}{q}\left(4p_f^2 - 3q^2\right)\log\left(\frac{2p_f+q}{2p_f-q}\right) - 2q^2\log\left(\frac{q^2-4p_f^2}{q^2}\right)\right] \tag{13}$$

and the remaining terms can be combined to give

$$q^2 + F^{vac}(q) = \frac{g^2}{48\pi^2}(11N - 2N_f)q^2\log\left(\frac{q^2}{\Lambda_{QCD}^2}\right) \tag{14}$$

Using Eqs. (1),(5),(12) and factoring out $\frac{g^2}{48\pi^2}$ by defining

$$D(q) \equiv \frac{g^2}{48\pi^2} f(q) \tag{15}$$

one finds:

$$V(r) \ = - \ \frac{6\left(N^2-1\right)}{Nr} Im \int_{-\infty}^{\infty} dq \frac{q e^{iqr}}{f(q)} \tag{16}$$

Thus, the potential $V(r)$ is independent of g^2. At zero temperature, the analytic structure of the gluon propagator is shown in Fig. 1b). Aside the branch cuts at $q = \pm 2p_f$, there is also a branch cut on the imaginary axis.

At zero density ($p_f = 0$), $F^{mat}(q)$ vanishes, and one has

$$f(q) = (11N - 2N_f)q^2\log\left(\frac{q^2}{\Lambda_{QCD}^2}\right) \tag{17}$$

Therefore, the gluon propagator has poles on the real axis (at $q = \pm\Lambda_{QCD}$), and the long-distance behavior of $V(r)$ is dominated by these poles. We have analyzed the behavior of this pole as p_f increases, for a chosen value of $\Lambda_{QCD} = 200$ MeV. First, the position of this pole shifts from the value of Λ_{QCD}, and a second pole at smaller q appears. However, for $p_f \gtrsim 120$ MeV both of them disappear and $1/D(q)$ will not have poles on the real axis. Since the deconfinement transition is thought to take place (at $T = 0$) at a density such that $p_f \gtrsim 300$ MeV, we can assume that no poles on the real axis will be present in the quark-gluon plasma phase. Instead, a pole with both a real and an imaginary part appears at $q_0 = q_r + iq_i$, as shown in Fig. 1b). This means that we have a situation similar to that encountered in the one-pion exchange, and we could have Yukawa-like oscillations. However, some remarks are in order. At zero temperature and $p_f \approx 300$ MeV we found $|q_0| \approx 200$ MeV, which is the value of Λ_{QCD}. This seems to invalidate our one-loop calculation, since we expect non-perturbative effects to be very large under these circumstances. Nevertheless, p_f introduces a new energy-scale into the problem (apart from Λ_{QCD}) and therefore the situation may be different for large values of p_f. In order to investigate this possibility, we have calculated the evolution of q_0 for increasing densities. The result can be seen in Fig. 5, where we have represented both the real part (solid line) and the imaginary part (dashed line) of q_0 as a function of

p_f (all units are in GeV). As one can see, for large values of p_f they become larger than Λ_{QCD}, making the perturbative expansion hopefully more reliable.

A similar situation appears if one keeps the density constant and increases the temperature. In this case, one has to recalculate Eq. (13) to take into account the temperature effects. The appropriate formulae can be found in [18], [19], [20]. We address the reader to these references and will not repeat here these formulae.

We have investigated the evolution of the Yukawa pole with temperature, for a fixed quark particle (minus antiparticle) density which corresponds to $p_f = 300$ MeV at $T = 0$. This is plotted in Fig. 6, where we followed similar conventions to the above figure, but now in the horizontal axis one has the temperature (in GeV). As we found before, large values of T makes the pole appear at large momenta. We made similar calculations starting from larger values of p_f and found no qualitative differences with the previous case. One expects the perturbative expansion to work better under these conditions. In fact, the asymptotic freedom property of QCD should manifest in this regime.

Let us now concentrate on the physical consequences of the analytic structure of the gluon propagator at $T = 0$ for the large-distances potential $V(r)$. By applying the residue theorem, the pole (Yukawa) contribution can be written as :

$$V_Y(r) = -\frac{24\pi(N^2-1)}{N\,(a^2+b^2)}\frac{\exp(-q_i r)}{r}\left[a\cos(q_r r) + b\sin(q_r r)\right] \tag{18}$$

where

$$\frac{f^{'}(q_0)}{q_0} \equiv a + ib \tag{19}$$

has to be calculated at the position of the pole . One has also to include the contribution to $V(r)$ coming from the branch cut running up the imaginary axis, which we will write as $V_{im}(r)$. At zero temperature and large distances, this contribution can be easily approximated (proceeding as in [10]) :

$$V_{im}(r\to\infty) \simeq \frac{(11N-2N_f)g^4}{32N\pi^3}\frac{(N^2-1)}{m_{el}^4 r^5} = \frac{\pi\,(11N-2N_f)}{8N}\frac{\left(N^2-1\right)}{N_f^2 p_f^4 r^5} \tag{20}$$

with the electric mass defined as

$$m_{el}^2 = D(q\to 0) = \frac{g^2 N_f p_f^2}{2\pi^2} \tag{21}$$

The contribution from the branch cuts at $q = \pm 2p_f$ (Friedel component) is similar to Eq. (11) (see [10]). In Fig. 7 we have plotted the different components of $V(r)$ (in MeV) mentioned above, at zero temperature and $p_f = 300$ MeV, as a function of the distance (in fm). The solid line gives the result of the numerical integration of Eq. (16) : we will call this the *exact* potential. The dotted line shows the Yukawa component, as given by Eq. (18) . Also shown is the contribution from Eq. (20) (long dashes) and the Friedel component, as given in Ref. [10] (short dashes). Finally, the dotted-dashed line is obtained by the sum of the Friedel, Yukawa and Eq. (20). As can be seen from this figure, the Yukawa component alone gives a reasonable approximation to $V(r)$ for this distance range. Also, it is clear that Eq. (20) overestimates the imaginary branch cut contribution for moderate distances. The Friedel component here is much smaller than the others.

The situation changes for larger distances. We have represented in Fig. 8 the same pieces of the potential, but for a distance range $r : 5 - 10$ fm. Now the contribution from $V_{im}(r)$ makes the approximate potential closer to the exact curve. This becomes apparent when we consider even a larger r , as seen in Fig. 9. For this range of distances, the Yukawa component tends to disappear, while Friedel oscillations are still important, so that the potential can be approximated by the Friedel and $V_{im}(r)$ contributions. Anyway, for distances $r \gtrsim 5$ fm, $V(r)$ becomes too small. For the distance range where the potential is of the order of a few MeV, it is reasonably approximated by the Yukawa component alone.

IV. CONCLUSIONS

In this work, we have considered plasma screening effects on the potential interaction for two static 'charges' in different models of dense matter. First, we studied the one-pion exchange in nuclear matter, as representative of QHD (Quantum Hadrodynamics). In addition to Friedel oscillations, which arise due to logarithmic branch cuts on the complex q-plane of the pion propagator, we find that this propagator shows a pole on this plane at zero temperature and densities above saturation. This pole gives rise to additional oscillations on the nucleon-nucleon potential, which we refer to as 'Yukawa oscillations'. In contrast to Friedel oscillations, which are damped as some power-law of the distance, Yukawa oscillations are exponentially damped with distance. Another important difference is the temperature behavior. While Friedel oscillations are strongly suppressed for temperatures of a few MeV, Yukawa oscillations are present up to $T \sim 60$ MeV when the density is equal to the saturation density. There is a critical temperature T_c for each density, below which Yukawa oscillations are present.

In order to investigate wether this phenomena are a peculiarity of this model or not, we have made further research. One feature of the pion exchange is the large value of the coupling constant. We considered the one-photon propagator in a QED plasma with an artificially increased value of the electromagnetic coupling constant. However, we found no Yukawa poles even if the coupling constant is taken to be of the order of unity or more. Thus, a large value of the coupling constant alone can not explain the origin of such pole.

Another important feature of QHD is that it shows no asymptotic freedom. This feature originates some pathologies in the meson sector, such as the appearance of tachyonich branches [24], [25]. Therefore, one might suspect that Yukawa poles are also a pathological behavior of non asymptotically-free field-nuclear models. In order to investigate this aspect, we have studied the singlet quark-antiquark potential in a QCD quark-gluon plasma. In the case we studied, Yukawa poles appear, at zero temperature, when the quark Fermi momentum reaches $p_f \gtrsim 120$ MeV and remain for larger densities. When the temperature is increased they survive, at least up to $T = 2$ GeV, which is the maximum temperature we reached in our calculations. This situation is in contrast with the one-pion model, where the pole disappears at some critical temperature. It is important to notice that, although the values of q at the pole are close to Λ_{QCD} for low densities and temperatures, they become large (as compared to Λ_{QCD}) if the density and/or temperature increases. Since one expects to obtain asymptotic freedom in this limit, a perturbative treatment like the one we have considered has more chances to be valid in these circumstances. In other words, Yukawa poles in a nuclear medium do not seem to be associated to non-asymptotically free theories and might correspond to some underlying physical phenomenon. As in the case of Friedel oscillations, this could manifest in the appearance of new phases in dense matter. Of course, they could also be a consequence of the approximations made in our models (namely the one-loop approximation) and might be not present in more realistic calculations. This will be the subject of a future work.

Acknowledgments

We are grateful to Drs. V. Vento and A. Nieto for fruitful discussions. This work has been partially supported by Spanish DGICYT Grant PB94-0973 and CICYT AEN96-1718.

---

[1] J.D. Bjorken, S. Drell, "Relativistic Quantum Fields". (McGraw-Hill, New York, 1965). S. Weinberg, "The Quantum Theory of Fields". (Cambridge Univ. Press, 1995).
[2] J. Friedel, *Phyl. Mag.* **43** (1952), 153. Nuovo Cim.**7** (1958), Suppl.2 287.
[3] H. Sivak, *Physica* **A129** (1985) 408.
[4] A. Delsante and N. E. Frankel, *Annals of Phys. (N.Y.)* **125** (1980) 135.
[5] T.J. Rowland, *Phys. Rev.* **V119** N3 (1960) 900.
[6] B.D. Serot, J.D. Walecka, "The Relativistic Nuclear Many-Body Problem", Adv. in Nucl. Phys., **16**, J.W. Negele and E. Vogt Edts. (Plenum, New York, 1986).
[7] R. Machleidt. "The Meson Theory of Nuclear Forces and Nuclear Structure." Adv. in Nucl. Phys. Vol.**19**; J.W. Negele and E. Vogt Edts. (Plenum, New York, 1989.)
[8] E. Gallego, J. Diaz Alonso, A. Pérez, *Nucl. Phys.* **A578** (1994) 542. J. Diaz Alonso, E. Gallego, A. Perez *Phys. Rev. Lett.* V.73; N.19; (1994); 2536.
[9] J. Diaz Alonso, A. Pérez, H. Sivak, *Nucl. Phys.* **A205** (1989) 695.
[10] J. Kapusta, T. Toimela, *Phys. Rev.* **D37** (1988) 3731.
[11] W. Kohn, Phys. Rev. Lett. **2** (1959) 393.
[12] S.A. Chin, Ann. Phys. **108** (1977) 301.

[13] H. Hakim, Riv. Nuovo Cimento **1** N6 (1978).
[14] J. Diaz Alonso, *Annals of Phys.*; V160; N1; (1985); 1.
[15] T. Matsui, B.D. Serot, Ann. Phys. **144**, N1, (1982), 107.
[16] J. Diaz Alonso, A. Pérez, *Nucl. Phys.* **A526** (1991) 623.
[17] M.P. Allendes, B.D. Serot, *Phys. Rev.* **C45** (1992) 2975. B.D. Serot, H.B. Tang, *Phys. Rev.* **C51** (1991) 969.
[18] J. Kapusta, "Finite-temperature field theory". Cambridge University Press, Cambridge (1989).
[19] K. Kajantie, J. Kapusta, *Annals of Phys.* **160** (1985) 477.
[20] T. Toimela, *Int. Jour. of Theor. Phys.* **24**, N9, (1985), 901.
[21] C. E. Price, J. R. Shepard and J. A. McNeil, *Phys. Rev.* **C 41**, *(1990) 1234.*
[22] C. E. Price, J. R. Shepard and J. A. McNeil, *Phys. Rev.* **C 42**, *(1990) 247.*
[23] M.J. Lighthill, "Introduction to Fourier Analysis and Generalized Functions" (Cambridge Univ. Press, Cambridge 1964).
[24] R. J. Perry *Phys. Lett. B 199, (1987), 489.*
[25] K. Wehrberger, R. Wittman and B. D. Serot, *Phys. Rev.* **C49,** *(1990), 2680.*

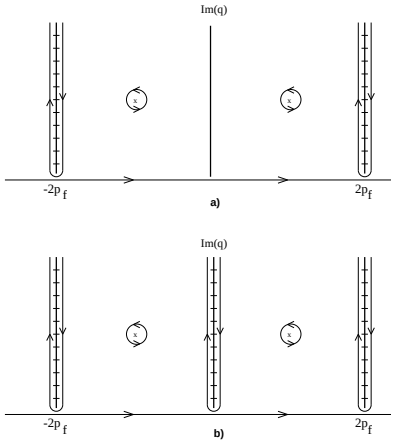

FIG. 1. Analytically-continued structure of the pion propagator (upper part) and gluon propagator (lower part) at zero temperature. Represented schematically are the contour paths used for integration. The Yukawa pole is indicated as an encircled cross.

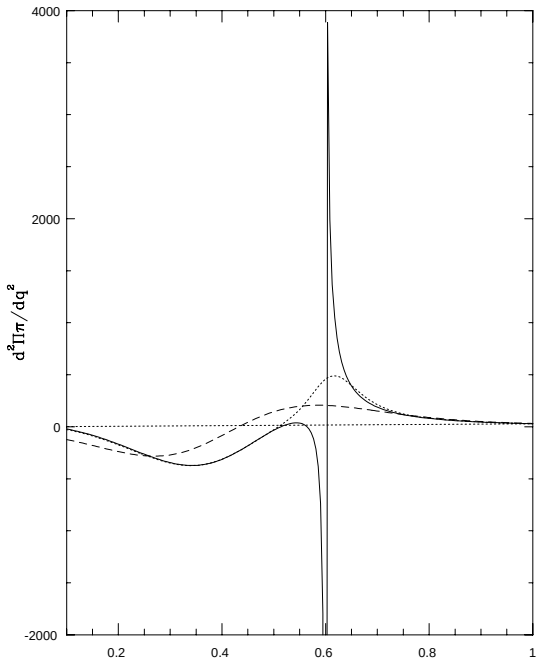

FIG. 2. Second derivative of the pion polarization as a function of q/m for three temperatures at saturation density : at zero temperature (solid curve) the Kohn singularity at $q = 2p_f$ is apparent. As temperature increases, the curve becomes smooth. We showed this behavior for $T = 5$ MeV (short dashes) and $T = 20$ MeV (long dashes).

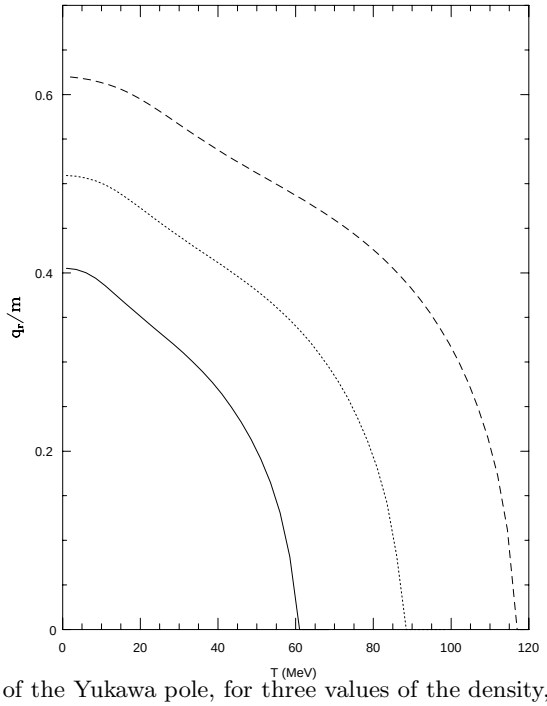

FIG. 3. Evolution of the real part of the Yukawa pole, for three values of the density, as temperature increases. The curves correspond to $p_f = 0.3$ (solid curve), $p_f = 0.35$ (dotted) and $p_f = 0.4$ (dashed), which are values of the nucleon Fermi momentum at $T = 0$.

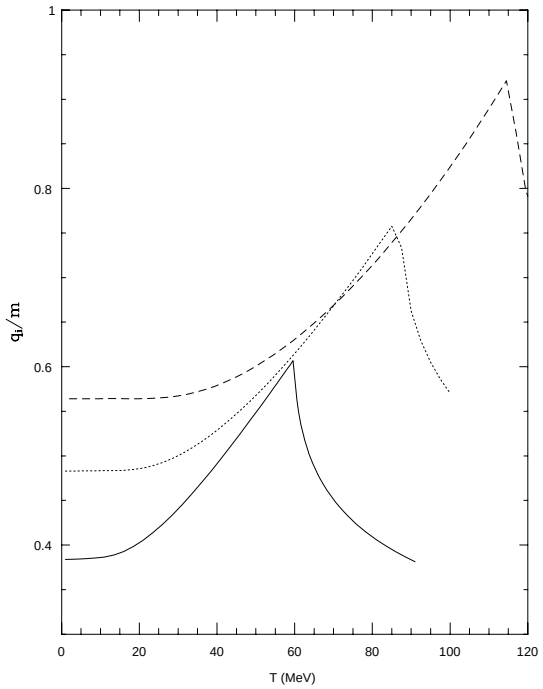

FIG. 4. Same as before, for the imaginary part of the pole.

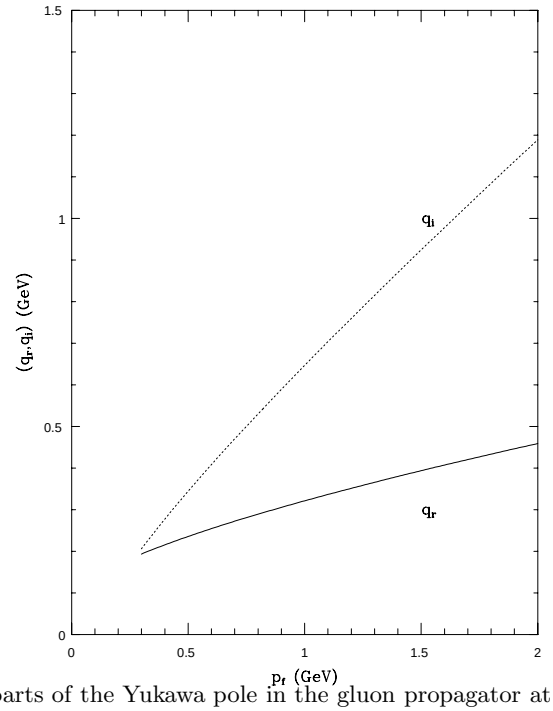

FIG. 5. The real and imaginary parts of the Yukawa pole in the gluon propagator at zero temperature, as a function of the quark Fermi momentum.

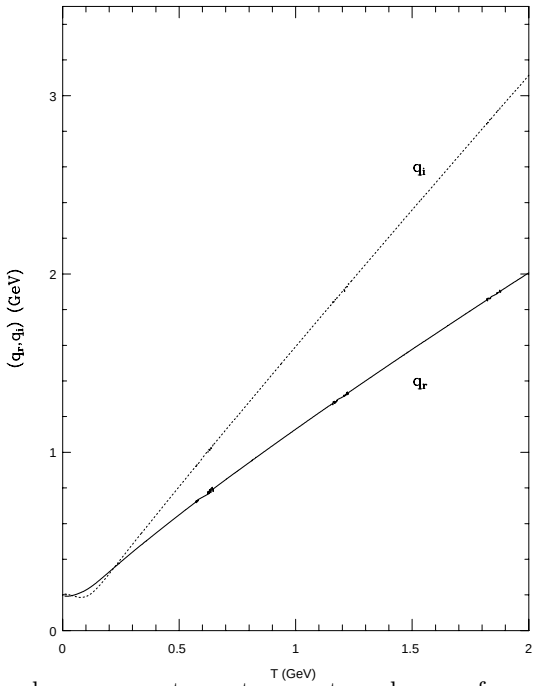

FIG. 6. Evolution of the pole of the gluon propagator as temperature changes, for a density corresponding to $p_f = 300$ MeV at $T = 0$.

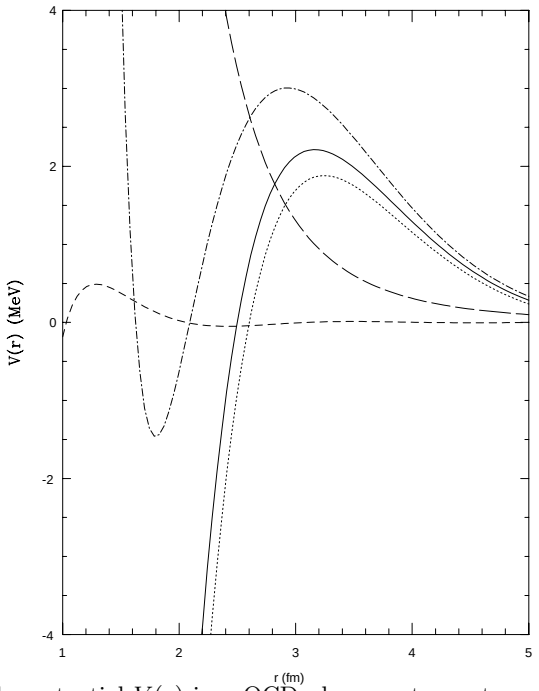

FIG. 7. Different components of the potential $V(r)$ in a QCD plasma, at zero temperature and $p_f = 300$ MeV. Solid line : result of the numerical integration of Eq. (16). The dotted line shows the Yukawa component, as given by Eq. (18) . Also shown is the contribution from Eq. (20) (long dashes) and the Friedel component (short dashes). Finally, the dotted-dashed line is obtained by the sum of the Friedel, Yukawa and Eq. (20).

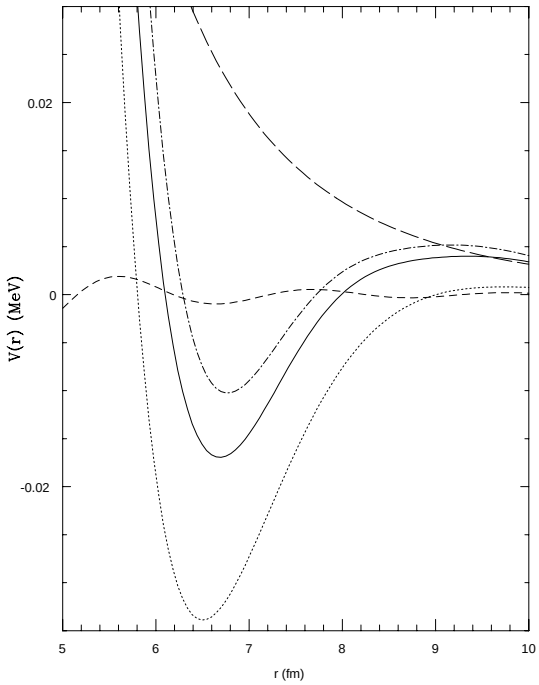

FIG. 8. Same as Fig. 7, for r between 5 and 10 fm.

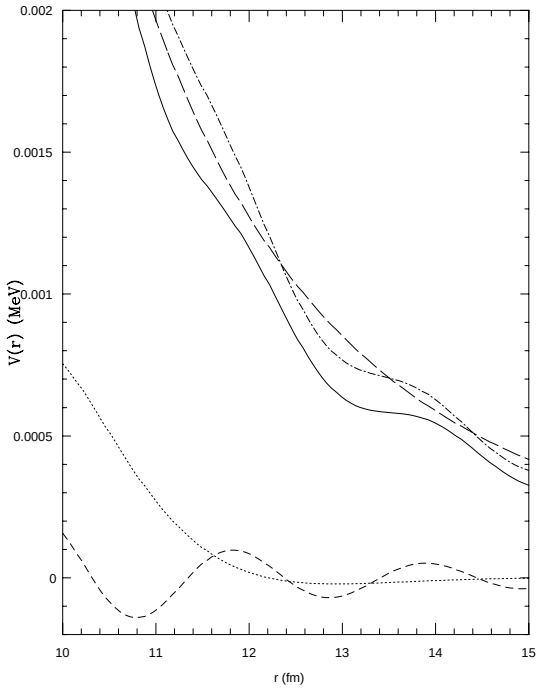

FIG. 9. Same as Fig. 7, for r between 10 and 15 fm.